

This is a repository copy of *Synthesis and evaluation of Fe₃O₄-impregnated activated carbon for dioxin removal*.

White Rose Research Online URL for this paper:

<https://eprints.whiterose.ac.uk/166279/>

Version: Accepted Version

Article:

Tu, Yao Jen, Premachandra, Gnanasiri S., Boyd, Stephen A. et al. (4 more authors) (2021) Synthesis and evaluation of Fe₃O₄-impregnated activated carbon for dioxin removal. CHEMOSPHERE. 128263. ISSN 0045-6535

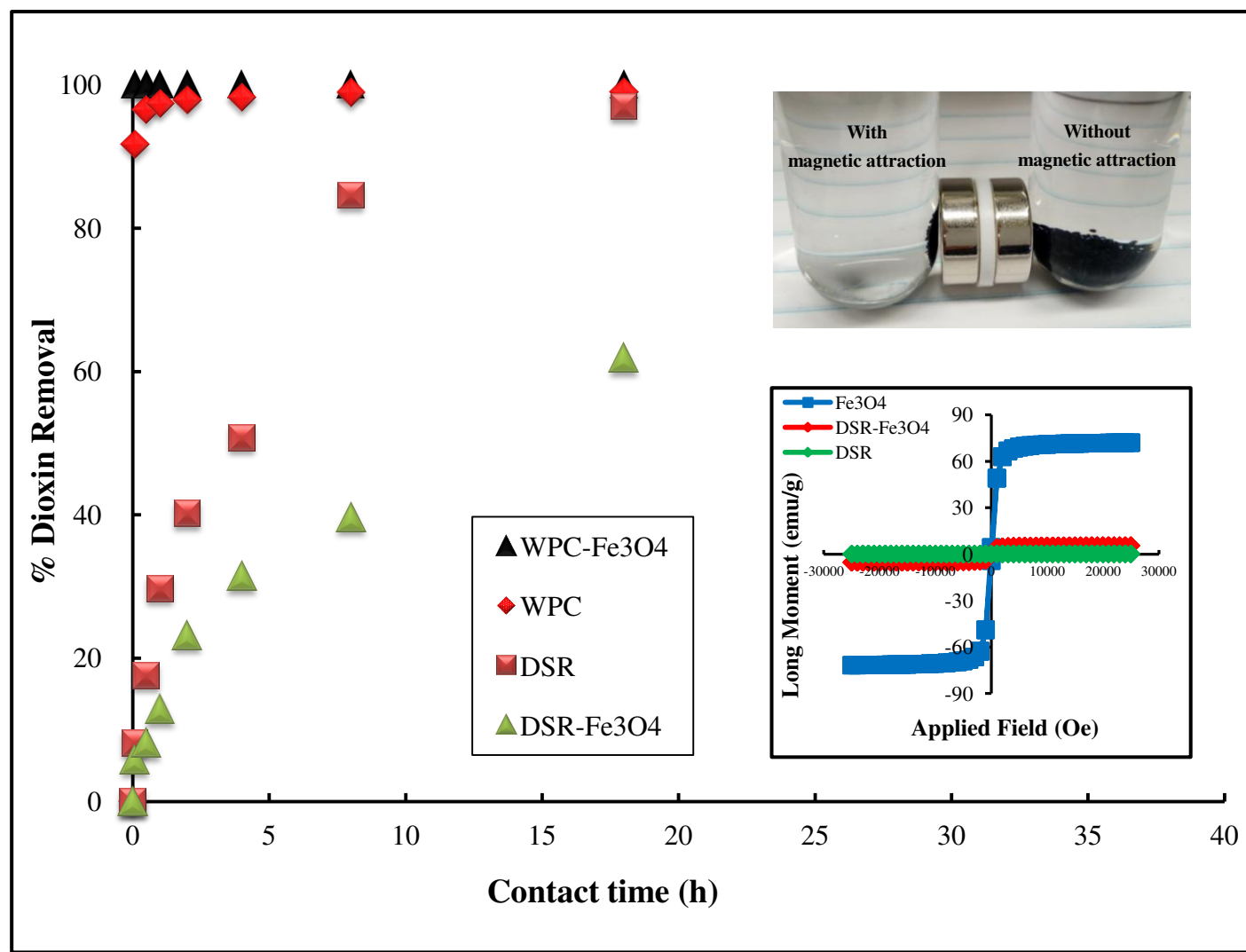
<https://doi.org/10.1016/j.chemosphere.2020.128263>

Reuse

This article is distributed under the terms of the Creative Commons Attribution-NonCommercial-NoDerivs (CC BY-NC-ND) licence. This licence only allows you to download this work and share it with others as long as you credit the authors, but you can't change the article in any way or use it commercially. More information and the full terms of the licence here: <https://creativecommons.org/licenses/>

Takedown

If you consider content in White Rose Research Online to be in breach of UK law, please notify us by emailing eprints@whiterose.ac.uk including the URL of the record and the reason for the withdrawal request.



Synthesis and evaluation of Fe₃O₄-impregnated activated carbon for dioxin removal

Yao-Jen Tu^a, Gnanasiri S. Premachandra^b, Stephen A. Boyd^c, J. Brett Sallach^d, Hui Li^c, Brian J. Teppen^c, Cliff T. Johnston^{b,c*}

^a School of Environmental and Geographical Sciences, Shanghai Normal University, 100 Guilin Rd. Shanghai, 200234, China

^b Department of Agronomy, Purdue University, 915 W. State Street, West Lafayette, Indiana 47907, USA

^c Department of Plant, Soil, and Microbial Sciences, Michigan State University, East Lansing, Michigan, 48824, USA

^d Department of Environment and Geography, University of York, Heslington, York, YO10 5NG, UK

^e Department of Earth, Atmospheric and Planetary Sciences, 550 Stadium Mall, Purdue University, West Lafayette, IN 47907, USA

Corresponding author: Cliff T. Johnston

Fax: +1-7654961716

E-mail: cliffjohnston@purdue.edu

1 Synthesis and evaluation of Fe₃O₄-impregnated activated carbon for dioxin removal

2

3 Yao-Jen Tu^a, Gnanasiri S. Premachandra^b, Stephen A. Boyd^c, J. Brett Sallach^d, Hui Li^c, Brian
4 J. Teppen^c, Cliff T. Johnston^{b,e*}

5

6 ^a School of Environmental and Geographical Sciences, Shanghai Normal University, 100

7 Guilin Rd. Shanghai, 200234, China

8 ^b Department of Agronomy, Purdue University, 915 W. State Street, West Lafayette, Indiana

9 47907, USA

10 ^c Department of Plant, Soil, and Microbial Sciences, Michigan State University, East Lansing,

11 Michigan, 48824, USA

12 ^d Department of Environment and Geography, University of York, Heslington, York, YO10

13 5NG, UK

14 ^e Department of Earth, Atmospheric and Planetary Sciences, 550 Stadium Mall, Purdue

15 University, West Lafayette, IN 47907, USA

16 Corresponding author: Cliff T. Johnston

17 Fax: +1-7654961716

18 E-mail: cliffjohnston@purdue.edu

19

20 **Abstract**

21 Polychlorinated dibenzo-p-dioxins and -furans (PCDD/PCDFs) are highly toxic organic
22 pollutants in soils and sediments which persist over timescales that extend from decades to
23 centuries. There is a growing need to develop effective technologies for remediating
24 PCDD/Fs-contaminated soils and sediments to protect human and ecosystem health. The use
25 of sorbent amendments to sequester PCDD/Fs has emerged as one promising technology. A
26 synthesis method is described here to create a magnetic activated carbon composite
27 (AC-Fe₃O₄) for dioxin removal and sampling that could be recovered from soils using
28 magnetic separation. Six AC-Fe₃O₄ composites were evaluated (five granular ACs (GACs)
29 and one fine-textured powder AC(PAC)) for their magnetization and ability to sequester
30 dibenzo-p-dioxin (DD). Both GAC/PAC and GAC/PAC-Fe₃O₄ composites effectively
31 removed DD from aqueous solution. The sorption affinity of DD for GAC-Fe₃O₄ was slightly
32 reduced compared to GAC alone, which is attributed to the blocking of sorption sites. The
33 magnetization of a GAC-Fe₃O₄ composite reached 5.38 emu/g based on SQUID results,
34 allowing the adsorbent to be easily separated from aqueous solution using an external
35 magnetic field. Similarly, a fine-textured PAC-Fe₃O₄ composite was synthesized with a
36 magnetization of 9.3 emu/g.

37

38 Keywords: dibenzo-p-dioxin, granular activated carbon, Fe₃O₄, magnetic separation,

39 activated carbon-Fe₃O₄ composite

40 **1. Introduction**

41 Polychlorinated dibenzo-p-dioxins (PCDDs) are prototypical persistent organic pollutants
42 (POPs) that are commonly found in soils and sediments. Due to their exceptionally low water
43 solubilities, these highly toxic lipophilic substances are highly bio-accumulative (Guruge et
44 al., 2005; Maier et al., 2016; Champoux et al., 2017). Exposure to PCDDs, even at trace
45 concentrations (Denison et al., 1989; Eljarrat et al., 2002), can result in measurable toxic and
46 carcinogenic effects in mammals (Huwe, 2002; McKay, 2002; Charnley and Doull, 2005).
47 PCDDs occur both naturally and from anthropogenic activities which include forest fires,
48 coal combustion, iron ore sintering, chlorine bleaching of pulp and paper, waste incineration,
49 and as by-products of pesticide manufacturing and the chlor-alkali process (Fiedler, 1996;
50 Everaert and Baeyens, 2002; Kulkarni et al., 2008; Zheng et al., 2008; Zhou et al., 2016;
51 Prisciandaroa et al., 2017; Zhao et al., 2017). Owing to their lipophilicity, PCDD/Fs
52 accumulate in surface soils, sediments and biota, including the fatty tissues of fish (WHO,
53 2010). In natural environments, they occur predominantly in the sorbed state associated with
54 pyrogenic carbonaceous matter (PCM), amorphous organic matter, and clays (Ferrario et al.,
55 2000; Fabietti et al., 2010). In fact, the significant role of PCM as a sorption domain has been
56 well established (Cornelissen et al., 2005). As a group, PCDD/Fs are characterized by low
57 aqueous solubilities and high octanol-water coefficients K_{ow} (Shiu et al., 1988; Kim et al.,

58 [2002; Li et al., 2009](#)). Consequently, their concentrations in natural waters are extremely low
59 with concentration ranges of pg/L to fg/L ([Charlestra et al., 2008; Cornelissen et al., 2008b;](#)
60 [Louchouarn et al., 2018](#)). PCDD/F-contaminated soils are found in ecosystems worldwide
61 ([Masunaga et al., 2001; Moon et al., 2008; Zheng et al., 2008](#)), and have proven difficult and
62 expensive to remediate. For example, the estimated cleanup cost of a *single* Superfund site
63 along the Passaic River which is contaminated by PCDD/Fs has exceeded one billion US
64 dollars.

65 Traditional site remediation has relied on removal of the contaminants via excavation or
66 dredging followed by disposal in a hazardous waste landfill. Recently, sorbent amendments
67 have gained attention as a means to lower or even eliminate bioavailability of soil/sediment-
68 bound contaminants ([Ghosh et al., 2011; Cornelissen et al., 2012; Hale et al., 2012;](#)
69 [Cornelissen et al., 2016; Cho et al., 2017](#)), and this has formed the basis of a new direction in
70 management of sites contaminated with PCDD/Fs ([Ghosh et al., 2011](#)). Activated carbon
71 (AC) materials (including granular activated carbon (GAC) and powdered activated carbon
72 (PAC), has emerged as an effective sorbent amendment for this purpose ([Cornelissen et al.,](#)
73 [2012; Denyes et al., 2013; Gomez-Eyles et al., 2013; Balasubramani and Rifai, 2018](#)).

74 The retrieval of the amendment with its sorbed contaminants after deployment has
75 become a priority for a number of reasons. First, complete removal of contaminants, rather
76 than just immobilization, is preferred by many environmental regulatory agencies ([e.g.,](#)

77 [USEPA, 1997](#)). Second, recovery of the sorbent amendment after its use as a passive sampler
78 can help determine mass transfer kinetics ([Cornelissen et al., 2008a](#); [Oen et al., 2011](#)).
79 Adsorbent magnetization is an emerging remediation area where magnetic separation
80 simplifies isolation and regeneration ([Mohan et al., 2014](#)). Numerous studies have
81 demonstrated that activated carbon/Fe₃O₄ composites can be synthesized that maintain high
82 surface area and high sorption affinities for a growing list of contaminants that includes
83 organic dyes ([Do et al., 2011](#)), arsenic ([Zhang et al., 2007](#), [Zhang et al., 2010](#)), heavy metals
84 ([Han et al., 2015](#)), pesticides and PAHs ([Mohan et al., 2014](#)). Our previous work showed
85 that magnetic Fe₃O₄ can be easily fabricated from the hydrothermal ferrite process and has
86 the potential to remove/recover toxic/precious elements from aqueous solutions ([Tu et al.,](#)
87 [2012](#); [Tu et al., 2013](#); [Tu et al., 2015](#)). To date, adsorbent magnetization has not been applied
88 to applications involving PCDD/Fs.

89 In our prior work, we provided the first evidence that bioavailability of TCDD sorbed to
90 two contrasting GACs and one PAC was eliminated in the mammalian (mouse) model. This
91 conclusion was based upon the use of two highly sensitive bioassays, hepatic induction of
92 cyp1A1 mRNA, an indirect measure of TCDD exposure, and immunoglobulin M antibody-
93 forming cell response, a direct measure of immune response ([Boyd et al., 2017](#); [Sallach et al.,](#)
94 [2019](#)). Prior to this, reductions in bioavailability had only been established based on simpler
95 model organisms (e.g., worms) or passive samplers ([Fagervold et al., 2010](#); [Chai et al., 2011](#);

96 [Chai et al., 2012](#)). Although the ACs represented a wide range of particle size and pore size
97 distributions, they were equally effective in eliminating the bioavailability of TCDD, making
98 them viable candidates for remediation. In this study, we pursued an additional line of
99 investigation to determine if these same ACs could be functionalized using *in situ* synthesis
100 of Fe₃O₄ for subsequent magnetic retrieval ([Indhu et al., 2015](#); [Choi et al., 2016](#)) without
101 compromising their affinity for dioxins.

102 AC-Fe₃O₄ composites were synthesized using the same GACs/PAC used in prior
103 bioavailability studies ([Boyd et al., 2017](#); [Sallach et al., 2019](#)). The specific goals of the
104 current work were to (1) synthesize GAC/PAC-Fe₃O₄ composites using ACs shown to be
105 effective in eliminating TCDD bioavailability in mammals, with emphasis on gaining new
106 physicochemical insight into the interaction between GAC/PAC and Fe₃O₄, (2) characterize
107 the composites using a combination of X-ray diffraction (XRD), scanning electron
108 microscopy (SEM), N₂-BET and micropore analysis, and superconducting quantum
109 interference device (SQUID); and (3) evaluate sorption characteristics (kinetics and
110 equilibration) of GAC/PAC, Fe₃O₄, and the GAC/PAC-Fe₃O₄ composite for aqueous phase
111 dibenzo-p-dioxin (DD). The compound DD served as an isostructural conservative surrogate
112 for PCDD/Fs, which are important targets for sequestration using environmental geosorbents
113 due to their extreme recalcitrance in natural environments ([Van Den Berg et al., 1998](#);
114 [Sallach et al., 2019](#); [Johnston et al., 2012](#)).

115 2. Materials and methods

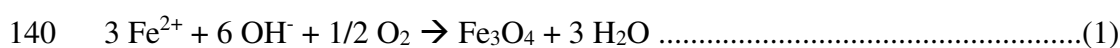
116 2.1. Chemicals and materials

117 All solutions were prepared with deionized water. Fe_3O_4 was synthesized from ferrous
118 sulfate FeSO_4 (> 99.9%, Fisher Scientific, USA) and sodium hydroxide NaOH (99.5%,
119 Fisher Scientific, USA). Dibenzo-p-dioxin (99% pure) was purchased from ChemService
120 (West Chester, PA, USA) and was used as received. All the reagents are of analytical grade
121 and used without further purification. Five GACs (DSRA, G60, FM-1, TOG-LF, and, F400)
122 and one fine textured PAC (WPC) were purchased/obtained from USEPA, Sigma Aldrich,
123 Cabot, Calgon Carbon Corp.,. Selected physical properties of the six GACs/PAC are given in
124 Table 1.

125 2.2. Synthesis procedure for magnetic AC- Fe_3O_4 composites

126 The magnetic GAC/PAC- Fe_3O_4 composite synthesis followed two synthesis procedures
127 modified from our previously published method (Tu et al., 2013). Method A was performed
128 using 0.01 M FeSO_4 at $T=338$ K, pH 10, and a reaction time of 2 h. Method B was carried
129 out using 0.1 M FeSO_4 at $T=298$ K, pH 10, and the same 2 h reaction time. Briefly, one gram
130 of GAC/PAC material was dried under vacuum at room temperature for 20 h using a vacuum
131 oven (Model 280 A, Fisher Scientific, USA). Dried GAC/PAC was then immersed in 0.01 M
132 (Method A) or 0.1 M (Method B) FeSO_4 solution (0.5 L) and mixed continuously at room
133 temperature for 20 h. After mixing, the pH was adjusted to 10 by dropwise addition of 0.1 M

134 NaOH and then air was bubbled to the solution to initiate the reaction. The synthesis
135 reactions were carried out at 338 K (Method A) or 298 K (Method B) for 2 h while
136 maintaining the pH at 10. Finally, the resultant AC-Fe₃O₄ material was rinsed 5x with DI
137 water to remove free Fe₃O₄, and successfully magnetized GAC/PAC-Fe₃O₄ composites was
138 separated from the solution via magnet. The corresponding synthetic reaction of Fe₃O₄ can be
139 described as Eq. 1 (Tu et al., 2013).



141 2.3. Characterization of AC-Fe₃O₄ composite

142 The crystal phases were determined by X-ray diffraction (XRD; X'Pert Pro, Philips,
143 Netherlands) using graphite monochromatic cobalt radiation over the 2θ range 10-80°. The
144 surface morphology and particle size were examined by scanning electron microscopy (SEM;
145 Nova NanoSEM, Oxford instruments, UK). The saturation magnetization of the adsorbent
146 was measured using a Superconducting Quantum Interference Device (SQUID
147 magnetometer; MPMS-3, Quantum Design, USA) at 300 ±1 K. N₂ BET and micropore
148 analysis was conducted using a Micromeritics 3Flex Multiport Chemi/Physi/Micropore
149 Analyzer.

150 2.4. Measurement of adsorption isotherm

151 Batch adsorption experiments were conducted in duplicate using five initial aqueous DD
152 concentrations (0.18, 0.3, 0.4, 0.6 and 0.8 mg/L) prepared by a serial dilution of 800 mg/L of

153 DD methanol stock solution. The amount of methanol in the aqueous solutions was 0.1%
154 which is considered to have minimal cosolvent effects. Aqueous solutions of DD were
155 sonicated for 60 min at room temperature in a water bath sonicator prior to mixing with the
156 GAC/PAC (Branson 120, Branson Ultrasonics, Danbury, CT, USA).

157 Two and half (2.5) mg of the adsorbent (GAC, PAC, GAC-Fe₃O₄, PAC-Fe₃O₄) was
158 placed in 30 mL Corex glass tubes (Kimble, Vineland, NJ, USA) with
159 polytetrafluoroethylene (PTFE)-lined screw caps, and mixed with a 30 mL aliquot of DD in
160 aqueous solutions (methanol 0.1 %). Control samples containing the initial aqueous DD
161 solutions 0.6 and 0.8 mg/L of DD solution without AC were prepared for calibration to
162 determine the losses of DD in the batch reactor. Measured values of DD in the control
163 samples ranged from 0.58 to 0.62 mg/L and 0.78 to 0.82 mg/L for the 0.6 and 0.8 mg/L DD
164 solutions, respectively. These results indicated that loss of DD to glassware can be ignored.
165 The suspensions were sonicated for 30 sec prior to shaking at a speed of 60 rpm in a rotary
166 shaker (Glas-Col, Terre Haute, IN, USA) at room temperature for 10-48 h to achieve the
167 apparent sorption equilibrium. The supernatant and adsorbent were separated by
168 centrifugation for GAC/PAC and by external magnetic field for GAC/PAC-Fe₃O₄
169 composites. An aliquot of 1.0 mL of supernatant and DD standards (0.0, 0.18, 0.3, 0.4, 0.6
170 and 0.8 mg/L) were transferred to HPLC vials. In order to prevent any sorption of DD by
171 HPLC vials, 0.5 mL of methanol (99.9%) was added to each vial prior to the addition of the

172 supernatant. HPLC vials containing supernatant and methanol were vortexed for 30 sec using
173 a digital mini-vortexer (VWR, Radnor, PA, USA). Samples were then analyzed for DD
174 concentrations by direct injection of 50 μ L into a Thermo Scientific high-performance liquid
175 chromatography (HPLC) system (Ultimate 3000) equipped with a UV detector and a 150 \times
176 4.60 mm 5 micron Luna 5 μ m C8(2) 100 Å column (S/N 514816-4). Isocratic elution was
177 performed using a mobile phase of 80% methanol: 20% water (v/v) with a flow rate of 1.0
178 mL/min and wavelength of 223 nm for detection.

179 The amount of DD sorbed (q_e , mg/kg) was calculated as the difference between the
180 amount initially added and that remaining in the solution after equilibration (Eq. 2):

181
$$q_e = \frac{(C_o - C_e) \times V}{m_{ads}} \dots \dots \dots (2)$$

182 where C_o and C_e are DD concentration in liquid phase at time zero and after equilibration
183 (mg/L), respectively; V is the solution volume used in DD adsorption (L); m_{ads} is GAC/PAC
184 mass (kg).

185 2.5. Desorption

186 Following collection of the supernatant after equilibrium had been reached, the remaining
187 supernatant was carefully decanted and the solid phase was re-suspended in a 30 mL solution
188 of 25% and 99.9% methanol and water (v/v). Tubes were sonicated for 30 sec prior to
189 shaking 24 h at 60 rpm to ensure equilibrium. Then, the supernatant and adsorbent were
190 separated by either centrifugation (GAC/PAC) or external magnetic field (GAC/PAC- Fe_3O_4

191 composite). Approximately 1.5 mL aliquots of supernatant and standards of 0.18, 0.3, 0.4, 0.6
192 and 0.8 mg/L were transferred to HPLC vials for HPLC analysis. The amount of DD
193 desorbed was calculated directly from the concentration of DD present in the supernatant
194 following equation Eq. 3:

195 Desorption efficiency = $\frac{C \times V}{X} \times 100\%$(3)

196 where C (mg/L) is the concentration of DD in the desorption solution, V (L) is the volume of
197 the desorption solution, and X (g) is the amount of DD adsorbed.

198

199 **3. Results and discussion**

200 3.1. Adsorbent characterization in GAC

201 Six activated carbon materials consisting of five granular activated carbon (GAC)
202 materials (F400, FM-1, G60, TOG-LF, and DSRA) and one fine textured powdered activated
203 carbon powder (PAC) (WPC) were functionalized with Fe₃O₄. Selected physical properties of
204 the six materials are given in Table 1. All but one of these GAC/PAC materials (DSRA)
205 were used in recent TCDD bioavailability studies and were found to be highly effective in
206 eliminating mammalian bioavailability of TCDD (Boyd et al., 2017; Sallach et al., 2019).

207 The activated carbon materials (Table 1) were functionalized using two different
208 magnetite synthesis methods. Given their large specific surface areas and micropore (0-2 nm
209 pores) volumes (Table 1), some magnetite synthesis was expected to occur in the micro- and

210 mesopores (2-50 nm pores) of the GAC/PAC, along with surface decoration of exterior
211 surfaces of the GAC/PAC particles rendering the GAC/PAC-Fe₃O₄ composites magnetic.
212 Fe₃O₄ synthesis Method A was performed at elevated temperature (338 K) using 0.01 M
213 FeSO₄. The resulting magnetization of the PAC-Fe₃O₄ composite was successful with a value
214 of 9.7 emu/g (Table 1). In contrast, observed magnetization values measured at 300 K for the
215 five GACs were weak with values of 0.61 (DSRA), 0.54 (FM-1), 0.49 (TOG-LF), 0.46 (G60)
216 and 0.35 (F-400) emu/g (Table 1). For comparison, the magnetization of Fe₃O₄ synthesized
217 using Synthesis Method A without GAC/PAC was 71.9 emu/g. Weak magnetization values
218 in the ranged of 0.35-0.61 emu/g were not sufficient to allow rapid magnetic separation.

219 Because the magnetization values resulting from synthesis Method A for the granular
220 activated carbon samples were weak (0.35-0.61 emu/g), the Fe₃O₄ synthesis procedure was
221 modified using synthesis Method B, which utilized a higher concentration of FeSO₄ (0.1 M)
222 and a lower temperature of 298 K. The granular activated carbon sample DSRA was selected
223 because it showed the highest level of magnetization among the five GAC materials
224 evaluated using Method A (Table 1). Synthesis Method B resulted in a DSRA-Fe₃O₄
225 composite with a significantly improved magnetization value of 5.38 emu/g (Table 1). No
226 residual magnetism was detected in either of the GAC(DSRA)-Fe₃O₄ (Synthesis Method B)
227 or PAC(WPC)/Fe₃O₄ (Synthesis Method A) composites indicating that these two materials
228 are superparamagnetic (Table 1). For simplicity, the GAC(DSRA)-Fe₃O₄ complex (using

229 Synthesis Method B) will be referred to as GAC-Fe₃O₄(B) and the PAC(WPC)-Fe₃O₄
230 complex (using Synthesis Method A) will be referred to as PAC-Fe₃O₄(A), where (A) and
231 (B) refer to Synthesis Methods A and B, respectively.

232 The GAC-Fe₃O₄(B) composite in aqueous suspension was efficiently recovered by
233 applying an external magnetic field. The complete (~100%) separation of the GAC-Fe₃O₄(B)
234 composite from solution using a magnet was achieved within only 20 seconds (Supplemental
235 Information Fig. S1). When the external magnetic field was removed, the GAC-Fe₃O₄(B)
236 composite could be readily dispersed again in water by physical shaking.

237 The XRD patterns of the GAC-Fe₃O₄(B) and PAC-Fe₃O₄(A) composites are shown in
238 Fig. 2. The observed diffraction peaks at d-spacings of 4.846, 2.968, 2.531, 2.423, 2.099,
239 1.713, 1.615, and 1.484 Å matched the XRD reflections of Fe₃O₄ (JCPDS file number 04-
240 007-9093). No other peaks were detected in the XRD pattern of the GAC-Fe₃O₄(B)
241 confirming that the only crystalline phase present is Fe₃O₄ nanoparticles in the GAC-
242 Fe₃O₄(B) composite. In addition to the Fe₃O₄ peaks, the PAC-Fe₃O₄(A) composite had small
243 peaks at 24.2, 31.0 and 58.5 °2θ.

244 Further characterization of the GAC and the GAC-Fe₃O₄(B) composite was provided by
245 SEM imaging of the two materials at different levels of magnification (Figs. 3a-3f). The
246 average bulk size of the GAC was ~1 mm with <5% passing through a 40 US Mesh sieve
247 (420 μm) (Fig. 3a); 'large' pores were observed ranging in size from several μm to >10 μm

248 (Figs. 3b and 3c). The synthesized Fe_3O_4 particles were observed to be spherical, and their
249 primary particle size ranged between 20 and 120 nm (Fig. 3d). From the SEM images it is
250 evident that the synthesized Fe_3O_4 nanoparticles were randomly distributed on the surfaces
251 and pores of the GAC particles (Fig. 3f).

252 3.2 N_2 BET and Textural Analysis

253 N_2 BET and micro-textural analysis of the activated carbon materials prior to magnetite
254 synthesis are presented in Table 1. The supplier of the activated carbon, feedstock, along with
255 N_2 BET surface area and micropore analysis are presented in Table 1. The five granular
256 activated carbon samples ranged in percentage micropore (0-2 nm) volume from 29 to 82%
257 of the total micropore and mesopore (2-50 nm) volume. The fine textured WPC powder had
258 very little mesoporosity with 91% of its pore volume in the micropore range. Of the six
259 samples, five were used in prior toxicology studies to assess TCDD bioavailability (Boyd et
260 al., 2017; Sallach et al., 2019). Although these ACs represented a wide range of particle size
261 and pore size distributions, they were equally effective in eliminating the bioavailability of
262 TCDD, making them viable candidates for remediation. After Fe_3O_4 synthesis, the specific
263 surface area of the GAC(DSRA)- Fe_3O_4 composite decreased from 822 to 633 m^2/g along
264 with a modest reduction in micropore volume (0.388 to 0.262 g/cc) indicative of some partial
265 pore blocking by the magnetite particles (Table 1).

266 3.3. Batch equilibrium sorption and kinetics

267 Batch sorption isotherms of dibenzo-p-dioxin (DD) to GAC and GAC-Fe₃O₄(B) are
268 shown in Fig. 4. Both GAC and GAC-Fe₃O₄ composite showed a high affinity for aqueous
269 phase DD at low equilibrium concentrations (<0.005 mg/L) up to a sorbed concentration
270 about of about 4000 mg/kg. At higher equilibrium concentrations (0.005-0.12 mg/L), sorption
271 isotherms showed some nonlinear behavior exhibiting high affinity at low equilibrium
272 concentration followed by an “S-shaped” response (Giles and Smith, 1974). The GAC-
273 Fe₃O₄(B) isotherm is shifted to higher equilibrium concentrations (i.e., lower affinity)
274 compared the GAC, however, both materials sorbed > 8000 mg/kg. These results could be
275 explained by sorption processes involving easily accessible external sites and less accessible
276 pores. Since Fe₃O₄ demonstrated no sorption affinity for DD, its presence within the GAC
277 composite likely blocked some sorption sites or access to certain pores manifesting a slight
278 decrease in DD affinity.

279 The kinetics of DD sorption by GAC and GAC-Fe₃O₄ composite were evaluated over a
280 period of 40 h using the batch equilibration method (described above) with initial aqueous
281 phase DD concentrations of 0.18, 0.4, and 0.8 mg/L (Fig. 5). Sorption kinetics of DD can be
282 separated into two phases. Initially, within the first 10 h, both GAC and GAC-Fe₃O₄
283 demonstrated comparatively rapid uptake of DD for all three initial concentrations. This was
284 followed by a slower phase (>50 h) to reach apparent equilibrium.

285 For the lower and intermediate initial DD concentrations of 0.18 and 0.4 mg/L, DD
286 uptake from aqueous solution by GAC was rapid and nearly complete within the first 10 h;
287 the percent DD removal approached 100 percent (Fig 5c-f). However, at the higher initial DD
288 concentration of 0.8 mg/L, there is a more gradual approach to apparent equilibrium over
289 time (Fig. 5a-b). For the initial concentrations of 0.18 and 0.4 mg/L, DD adsorption by GAC
290 was essentially complete by 10 h, and the total uptake of DD from aqueous solution
291 approached 100 percent. For the initial concentration of 0.8 mg/L the data indicate that
292 equilibrium had not been achieved after 50 h for GAC-Fe₃O₄.

293 For this system, it is assumed that sorption kinetics are controlled surface adsorption with
294 associated resistance to film diffusion followed by an emerging contribution to DD sorption
295 via intraparticle diffusion. Pseudo-second order kinetic models are commonly used to
296 describe sorption kinetics for these types of interactions (Ho and, McKay, 1999;
297 Amarasinghe and Williams, 2007). The pseudo-second order kinetic model was able to fit
298 the experimental data well (see Table 2). The pseudo-second order model results are plotted
299 on the kinetics data shown in Fig. 5.

300 The correlation coefficients (R^2) and kinetic parameters derived from the pseudo-second
301 order models are summarized in Table 2. These results suggest that the rate-limiting step may
302 be some type of site-specific mechanism involving direct interaction between the sorbent and
303 sorbate (Amarasinghe and Williams, 2007). The kinetic rate constant (k_2) from the pseudo-

304 second order model decreased with increasing initial DD concentrations (Table 1), indicating
305 that the DD adsorption rates are faster at lower concentrations. In other words, the time
306 required to reach equilibrium increased as the initial DD concentration increased. This is
307 likely due to competition for active surface sites and pores of the sorbent which is greater at a
308 higher DD concentration.

309 3.4 Desorption of DD

310 Desorption of DD into solutions of either 25% or 99.9% methanol and water (v/v)
311 desorption solutions were used to evaluate the reversibility of DD sequestration by GAC and
312 the GAC-Fe₃O₄ composite. Desorption of DD from GAC and GAC-Fe₃O₄ in 99.9% methanol
313 was 19% and 14.3% (after 20 h), respectively, and 11.2% and 12.4% for 25%
314 methanol/water, respectively. These results agree with our prior study that showed 22-27%
315 of TCDD bound to three of the activated carbons samples used in the present study could be
316 desorbed after 64 hours of Soxhlet extraction using toluene (Sallach et al., 2019).
317 Magnetizing GAC with Fe₃O₄ had little to no effect on the propensity of DD to desorb. That
318 the fraction of released DD was less than 20% even for 99.9% methanol clearly indicated the
319 strong affinity between DD and GAC; once sorbed DD appears to be largely irreversibly-
320 sequestered within the pore structure of GAC. The resistance to desorption, even into
321 methanol, is consistent with our prior observation that sequestration of 2,3,7,8-TCDD by AC
322 eliminated its mammalian bioavailability (Boyd et al., 2017; Stedtfeld et al., 2017).

323 3.5 Sorption removal comparison of fine-textured AC-Fe₃O₄ to GAC-Fe₃O₄

324 The uptake of DD by GAC, GAC-DSR-Fe₃O₄(B), PAC and PAC-Fe₃O₄(A) as a function
325 of time are shown in Fig. 6. As expected, uptake of DD by the fine-textured AC (WPC) was
326 rapid and nearly stoichiometric. More than 90% of the WPC has a particle size of < 45 μm
327 (Sallach et al., 2019). In contrast, sorption kinetics for DD uptake by the coarse-textured
328 GAC and GAC-Fe₃O₄(B) were considerably slower. Although the surface area of the PAC,
329 GAC and their Fe₃O₄ derivatives are comparable, most of the surface area in GAC can only
330 be accessed through intraparticle diffusion, resulting in slower sorption kinetics (Figs. 5-6).

331 4. Discussion

332 The activated carbon materials, including GAC and PAC, used here to form the magnetic
333 variants were also used in our prior bioavailability studies (Boyd et al., 2017; Stedtfeld et al.,
334 2017; Sallach et al., 2019), along with natural geosorbents including clay minerals and silica
335 (Boyd et al., 2011; Kaplan et al., 2011; Chai et al., 2016). Among these, only GAC and PAC
336 eliminated the bioavailability of sorbed TCDD to a mammalian (mouse) model.
337 Mammalian bioavailability was evaluated in our prior work using two highly sensitive
338 bioassays, hepatic induction of cyp1A1 mRNA, an indirect measure of TCDD exposure, and
339 immunoglobulin M antibody-forming cell response, a direct measure of immune response
340 (Boyd et al., 2017; Sallach et al., 2019). In contrast to the complete elimination of TCDD
341 bioavailability achieved via sequestration by GAC/PAC, TCDD bound to clay minerals and

342 silica was found to be 100% bioavailable. The lack of mammalian bioavailability of TCDD
343 bound to GAC/PACs was consistent with a related study showing contaminant bioavailability
344 to lower organisms was significantly decreased in the presence of AC (Chai et al., 2012). In
345 addition, attempts to extract sorbed TCDD from ACs using Soxhlet extraction revealed that
346 only a minor fraction of the total TCDD present could be recovered (Sallach et al., 2019).
347 From an applied perspective, these laboratory results are now leading to the use of GAC/PAC
348 sorbent amendments in large-scale remediation efforts for impacted soils, sediments and
349 water bodies (Samuelsson et al., 2017; Payne et al., 2019; Cornelissen et al., 2016;
350 Beckingham et al., 2011). Given our earlier results showing elimination of mammalian
351 TCDD bioavailability, creating magnetic GAC/PAC composites that could be used as a
352 retrievable form of GAC/PAC sorbent amendments was attempted. The ability to retrieve
353 magnetized GAC/PAC would enhance their utility as passive samplers in field settings and in
354 ongoing laboratory studies. For example, our earlier mammalian studies would have
355 benefited from using a magnetic AC to determine the amount TCDD in fecal pellets from
356 mice that were dosed with TCDD–AC (Boyd et al., 2017; Stedfeldt et al., 2017; Sallach et al.,
357 2018). Likewise, the ability to ultimately retrieve (magnetized) GAC/PAC sorbent
358 amendments used to remediate areas with especially high levels of contamination would
359 provide both an immediate benefit, i.e., bioavailability reduction, and make contaminant
360 removal possible in the longer term.

361 The synthesis procedure using a lower concentration of FeSO_4 (0.01 M) at an elevated
362 temperature (338 K), Synthesis Method A, was successful in synthesizing a magnetic PAC-
363 Fe_3O_4 composite (PAC- Fe_3O_4 (A)). In the case of the PAC, magnetization most likely
364 occurs on the external surfaces of fine-textured AC and this could be accomplished using the
365 lower concentration of FeSO_4 . However, Method A only produced weak magnetization
366 values for the GAC- Fe_3O_4 composites. One could argue that this procedure was not able to
367 synthesize Fe_3O_4 particles within the coarse textured GACs. The procedure was modified
368 using a higher concentration of FeSO_4 (0.1 M) and lower temperature that resulted in a
369 sufficiently magnetic GAC- Fe_3O_4 (B) composite.

370 Both the GAC- Fe_3O_4 (B) and PAC- Fe_3O_4 (A) composites revealed the presence of Fe_3O_4
371 based on X-ray diffraction analysis (Fig. 2) and it is possible that careful XRD studies could
372 be used as a surrogate for the more difficult to obtain SQUID magnetization results. N_2 BET
373 surface area and textural analysis showed that both the GAC and PAC materials were
374 characterized by high N_2 -surface area (802-822 m^2/g). The specific surface area of the
375 GAC- Fe_3O_4 (B) composite showed a modest reduction in both surface area (822 to 633 m^2/g)
376 and micropore volume (0.38 g/cc to 0.26 g/cc) compared to the starting GAC (Table 1).
377 The batch sorption isotherms of dibenzo-p-dioxin (DD) on the GAC and GAC- Fe_3O_4 (B)
378 composites showed that sorption affinity of DD was slightly reduced due to the presence of
379 magnetite particles (GAC- Fe_3O_4 (B)) compared GAC. The decrease in surface area and DD

380 sorption is interpreted as some blocking of pore throats. Overall, the sorption isotherms for
381 both GAC and GAC-Fe₃O₄(B) showed some sorption nonlinearity, consistent with a range of
382 sorption sites of varying accessibility.

383 The sorption kinetics of DD uptake by GAC, GAC-Fe₃O₄(B), PAC and PAC-Fe₃O₄(A)
384 were strongly dependent on particle size. Uptake of DD by the fine textured PAC and PAC-
385 Fe₃O₄(A) composite was rapid and complete within 10 hours. In contrast, sorption uptake
386 was much slower for GAC and the GAC-Fe₃O₄(B) composite (Fig. 4 and 5) owing to the
387 larger particle size. Sorption equilibria had not been reached for the GAC-Fe₃O₄(B)
388 composite after 40 h. These results are consistent with prior work showing the influence of
389 particle size on sorption kinetics of hydrophobic organic solutes on activated carbon and
390 biochars (Ahn et al., 2005; Kang et al., 2018). As shown, the rate of DD uptake by the fine
391 textured AC and AC-Fe₃O₄(A) is rapid with showing 97% removal of DD from aqueous
392 solution after one hour. The larger sized GAC, with particle diameters ~ 1 mm (5% < 420
393 μm), showed much slower uptake (Fig. 6a) and is attributed to the longer diffusion pathways
394 to binding sites and pore structures in GAC.

395 We demonstrated that both a GAC and a PAC could be magnetized and, more
396 importantly, the GAC-Fe₃O₄(B) and PAC-Fe₃O₄(A) composites maintained high sorption
397 affinity for dioxin. Particle size was a dominant factor in controlling sorption kinetics, with
398 the fine-textured PAC showing nearly complete uptake of dioxin within 1 hour compared to

399 considerably slower uptake by the coarse texture GAC. These differences could be significant
400 in animal dosing studies but less significant for materials deployed as passive samplers over
401 periods of months to years. Finally, these results could prove useful in the design of large-
402 scale recoverable geosorbents manufactured for contaminant removal.

403 **Acknowledgments**

404 Research reported in this paper was supported by the National Institute of Environmental
405 Health Sciences and Shanghai Natural Science Foundation under Award Number
406 P42ES004911 and 20ZR1441100, respectively. The content is solely the responsibility of the
407 authors and does not necessarily represent the official views of the National Institutes of
408 Health. The authors appreciate Dr. Timothy Henderson and Dr. Neil R. Dilley (Birck
409 Nanotechnology Center) for their support with SEM and SQUID analysis.

410

411 **References**

- 412 Ahn, S., Werner, D., Karapanagioti, H.K., McGlothlin, D.R., Zare, R.N., Luthy, R.G., 2005.
413 Phenanthrene and pyrene sorption and intraparticle diffusion in polyoxymethylene, coke,
414 and activated carbon. *Environ. Sci. Technol.* 39, (17), 6516-6526.
- 415 Amarasinghe, B.M.W.P.K., Williams, R.A., 2007. Tea waste as a low cost adsorbent for Cu
416 and Pb removal from wastewater. *Chem. Eng. J.* 132, 299-309.
- 417 Balasubramani, A., Rifai, H.S., 2018. Efficacy of carbon-based materials for remediating

418 polychlorinated biphenyls (PCBs) in sediment. *Sci. Total Environ.* 644, 398-405.

419 Beckingham, B., Ghosh, U., 2011. Field-Scale Reduction of PCB Bioavailability with
420 Activated Carbon Amendment to River Sediments. *Environmental Science & Technology*
421 45, 10567-10574.

422 Boyd, S.A., Johnston, C.T., Pinnavaia, T.J., Kaminski, N.E., Teppen, B.J., Li, H., Khan, B.,
423 Crawford, R.B., Kovalova, N., Kim, S.S., Shao, H., Gu, C., Kaplan, B.L.F., 2011.
424 Suppression of humoral immune responses by 2,3,7,8-tetrachlorodibenzo-p-dioxin
425 intercalated in smectite clay. *Environ. Toxicol. Chem.* 30, (12), 2748-2755.

426 Boyd, S.A., Sallach, J.B., Zhang, Y., Crawford, R., Li, H., Johnston, C.T., Teppen, B.J.,
427 Kaminski, N.E., 2017. Sequestration of 2,3,7,8-tetrachlorodibenzo-p-dioxin by activated
428 carbon eliminates bioavailability and the suppression of immune function in mice.
429 *Environ. Toxicol. Chem.* 36, 2671-2678.

430 Champoux, L., Rail, J.F., Lavoie, R.A., 2017. Polychlorinated dibenzo-p-dioxins,
431 dibenzofurans, and flame retardants in northern gannet (*Morus bassanus*) eggs from
432 Bonaventure Island, Gulf of St. Lawrence, 1994-2014. *Environ. Pollut.* 222, 600-608.

433 Charlestra, L., Courtemanch, D.L., Amirbahman, A., Patterson, H., 2008. Semipermeable
434 membrane device (SPMD) for monitoring PCDD and PCDF levels from a paper mill
435 effluent in the Androscoggin River, Maine, USA. *Chemosphere* 72, 1171-1180.

436 Chai, B.L., Tsoi, T.V., Iwai, S., Liu, C., Fish, J.A., Gu, C., Johnson, T.A., Zylstra, G., Teppen,

437 B.J., Li, H., Hashsham, S.A., Boyd, S.A., Cole, J.R., Tiedje, J.M., 2016. *Sphingomonas*
438 *wittichii* strain RW1 genome-wide gene expression shifts in response to dioxins and clay.
439 *Plos One* 11, (6), 14.

440 Chai, Y.Z., Currie, R.J., Davis, J.W., Wilken, M., Martin, G.D., Fishman, V.N., Ghosh, U.,
441 2012. Effectiveness of activated carbon and biochar in reducing the availability of
442 polychlorinated dibenzo-p-dioxins/dibenzofurans in soils. *Environ. Sci. Technol.* 46 (2),
443 1035-1043.

444 Chai, Y.Z., Davis, J.W., Wilken, M., Martin, G.D., Mowery, D.M., Ghosh, U., 2011. Role of
445 black carbon in the distribution of polychlorinated dibenzo-p-dioxins/dibenzofurans in
446 aged field-contaminated soils. *Chemosphere* 82 (5), 639-647.

447 Charnley, G., Doull, J., 2005. Human exposure to dioxins from food, 1999-2002. *Food Chem.*
448 *Toxicol.* 43, 671-679.

449 Cho, D.W., Yoon, K., Kwon, E.E., Biswas, J.K., Song, H., 2017. Fabrication of magnetic
450 biochar as a treatment medium for As(V) via pyrolysis of FeCl₃-pretreated spent coffee
451 ground. *Environ. Pollut.* 229, 942-949.

452 Choi, Y.J., Wu, Y.W., Sani, B., Luthy, R.G., Werner, D., Kim, E., 2016. Performance of
453 retrievable activated carbons to treat sediment contaminated with polycyclic aromatic
454 hydrocarbons. *J. Hazard. Mater.* 320, 359-367.

455 Cornelissen, G., Amstaetter, K., Hauge, A., Schaanning, M., Beylich, B., Gunnarsson, J.S.,

456 Breedveld, G.D., Oen, A.M.P., Eek, E., 2012. Large-scale field study on thin-layer
457 capping of marine PCDD/F-contaminated sediments in Grenlandfjords, Norway:
458 physicochemical effects. *Environ. Sci. Technol.* 46, 12030-12037.

459 Cornelissen, G., Arp, H.P.H., Pettersen, A., Hauge, A., Breedveld, G.D., 2008a. Assessing
460 PAH and PCB emissions from the relocation of harbour sediments using equilibrium
461 passive samplers. *Chemosphere* 72, 1581-1587.

462 Cornelissen, G., Gustafsson, O., Bucheli, T.D., Jonker, M.T.O., Koelmans, A.A., Van Noort,
463 P.C.M., 2005. Extensive sorption of organic compounds to black carbon, coal, and
464 kerogen in sediments and soils: Mechanisms and consequences for distribution,
465 bioaccumulation, and biodegradation. *Environ. Sci. Technol.* 39, 6881-6895.

466 Cornelissen, G., Schaanning, M., Gunnarsson, J.S., Eek, E., 2016. A large-scale field trial of
467 thin-layer capping of PCDD/F-contaminated sediments: sediment-to-water fluxes up to 5
468 years post-amendment. *Integr. Environ. Assess. Manag.* 12, 216-221.

469 Cornelissen, G., Wiberg, K., Broman, D., Arp, H.P.H., Persson, Y., Sundqvist, K., Jonsson, P.,
470 2008b. Freely dissolved concentrations and sediment-water activity ratios of PCDD/Fs
471 and PCBs in the open Baltic Sea. *Environ. Sci. Technol.* 42, 8733-8739.

472 Denison, M.S., Fisher, J.M., Whitlock Jr, J.P., 1989. Protein-DNA interactions at recognition
473 sites for the dioxin-Ah receptor complex. *J. Biol. Chem.* 264, 16478-16482.

474 Denyes, M.J., Rutter, A., Zeeb, B.A., 2013. In situ application of activated carbon and biochar

475 to PCB-contaminated soil and the effects of mixing regime. *Environ. Pollut.* 182, 201-208.

476 Do, M.H., Phan, N.H., Nguyen, T.D., Thi, T.S.P., Nguyen, V.K., Thi, T.T.V., Thi, K.P.N.,
477 2011. Activated carbon/Fe₃O₄ nanoparticle composite: Fabrication, methyl orange
478 removal and regeneration by hydrogen peroxide. *Chemosphere* 85, 1269-1276.

479 Eljarrat, E., Monjonell, A., Caixach, J., Rivera, J., 2002. Toxic potency of polychlorinated
480 dibenzo-p-dioxins, polychlorinated dibenzofurans, and polychlorinated biphenyls in food
481 samples from Catalonia (Spain). *J. Agric. Food Chem.* 50, 1161-1167.

482 Everaert, K., Baeyens, J., 2002. The formation and emission of dioxins in large scale thermal
483 processes. *Chemosphere* 46, 439-448.

484 Fabietti, G., Biasioli, M., Barberis, R., Ajmone-Marsan, F., 2010. Soil contamination by
485 organic and inorganic pollutants at the regional scale: The case of piedmont, Italy. *J. Soil.*
486 *Sediment.* 10, 290-300.

487 Fagervold, S.K., Chai, Y.Z., Davis, J.W., Wilken, M., Cornelissen, G., Ghosh, U., 2010.
488 Bioaccumulation of polychlorinated dibenzo-p-dioxins/dibenzofurans in *E. fetida* from
489 floodplain soils and the effect of activated carbon amendment. *Environ. Sci. Technol.* 44
490 (14), 5546-5552.

491 Ferrario, J.B., Byrne, C.J., Cleverly, D.H., 2000. 2,3,7,8-dibenzo-p-dioxins in mined clay
492 products from the united states: Evidence for possible natural origin. *Environ. Sci.*
493 *Technol.* 34, 4524-4532.

494 Fiedler, H., 1996. Sources of PCDD/PCDF and impact on the environment. *Chemosphere* 32,
495 55-64.

496 Ghosh, U., Luthy, R.G., Cornelissen, G., Werner, D., Menzie, C.A., 2011. In situ sorbent
497 amendments: A new direction in contaminated sediment management. *Environ. Sci.*
498 *Technol.* 45, 1163-1168.

499 Giles, C.H., Smith, D., Huitson, A., 1974. A general treatment and classification of the solute
500 adsorption isotherm. I. Theoretical. *Journal of Colloid and Interface Science* 47, 755-765.

501 Gomez-Eyles, J.L., Yupangui, C., Beckingham, B., Riedel, G., Gilmour, C., Ghosh, U., 2013.
502 Evaluation of biochars and activated carbons for in-situ remediation of sediments
503 impacted with organics, mercury, and methylmercury. *Environ. Sci. Technol.* 47, 13721-
504 13729.

505 Guruge, K.S., Seike, N., Yamanaka, N., Miyazaki, S., 2005. Polychlorinated dibenzo-p-dioxins,
506 -dibenzofurans, and biphenyls in domestic animal food stuff and their fat. *Chemosphere*
507 58, 883-889.

508 Hale, S.E., Elmquist, M., Brandli, R., Hartnik, T., Jakob, L., Henriksen, T., Werner, D.,
509 Cornelissen, G., 2012. Activated carbon amendment to sequester PAHs in contaminated
510 soil: A lysimeter field trial. *Chemosphere* 87, 177-184.

511 Han, Z.T., Sani, B., Mrozik, W., Obst, M., Beckingham, B., Karapanagioti, H.K. Werner, D.,
512 2015. Magnetite impregnation effects on the sorbent properties of activated carbons and

513 biochars. *Water Res.* 70, 394-403.

514 Ho, Y.S., McKay, G., 1999. Pseudo-second order model for sorption processes. *Process*
515 *Biochem.* 34, 451-465.

516 Huwe, J.K., 2002. Dioxins in food: a modern agricultural perspective. *J. Agric. Food. Chem.*
517 50, 1739-1750.

518 Indhu, Z.T., Sani, B., Akkanen, J., Abel, S., Nybom, I., Karapanagioti, H.K., Werner, D., 2015.
519 A critical evaluation of magnetic activated carbon's potential for the remediation of
520 sediment impacted by polycyclic aromatic hydrocarbons. *J. Hazard. Mater.* 286, 41-47.

521 Johnston, C.T., Khan, B., Barth, E.F., Chattopadhyay, S., Boyd, S.A., 2012. Nature of the
522 interlayer environment in an organoclay optimized for the sequestration of dibenzo-p-
523 dioxin. *Environ. Sci. Technol.* 46, 9584-9591.

524 Kang, S., Jung, J., Choe, J.K., Ok, Y.S., Choi, Y., 2018. Effect of biochar particle size on
525 hydrophobic organic compound sorption kinetics: Applicability of using representative
526 size. *Sci. Total Environ.* 619, 410-418.

527 Kaplan, B.L.F., Crawford, R.B., Kovalova, N., Arencibia, A., Kim, S.S., Pinnavaia, T.J., Boyd,
528 S.A., Teppen, B.J., Kaminski, N.E., 2011. TCDD adsorbed on silica as a model for TCDD
529 contaminated soils: Evidence for suppression of humoral immunity in mice. *Toxicology*
530 282, (3), 82-87.

531 Kim, H.K., Masaki, H., Matsumur, T., Kamei, T., Magara, Y., 2002. Removal efficiency and

532 homologue patterns of dioxins in drinking water treatment. *Water Res.* 36, 4861-4869.

533 Kulkarni, P.S., Crespo, J.G., Afonso, C.A.M., 2008. Dioxins sources and current remediation
534 technologies-a review. *Environ. Int.* 34, 139-153.

535 Li, X.M., Peng, P.A., Zhang, S.K., Man, R., Sheng, G.Y., Fu, J.M., 2009. Removal of
536 polychlorinated dibenzo-p-dioxins and polychlorinated dibenzofurans by three coagulants
537 in simulated coagulation processes for drinking water treatment. *J. Hazard. Mater.* 162,
538 180-185.

539 Louchouart, P., Seward, S.M., Cornelissen, G., Arp, H.P.H., Yeager, K.M., Brinkmeyer, R.,
540 Santschi, P.H., 2018. Limited mobility of dioxins near San Jacinto super fund site (waste
541 pit) in the Houston Ship Channel, Texas due to strong sediment sorption. *Environ. Pollut.*
542 238, 988-998.

543 Maier, D., Benisek, M., Blaha, L., Dondero, F., Giesy, J.P., Köhler, H.R., Richter, D., Scheurer,
544 M., Tribskorn, R., 2016. Reduction of dioxin-like toxicity in effluents by additional
545 wastewater treatment and related effects in fish. *Ecotoxicol. Environ. Saf.* 132, 47-58.

546 Masunaga, S., Yao, Y., Ogura, I., Nakai, S., Kanai, Y., Yamamuro, M., Nakanishi, J., 2001.
547 Identifying sources and mass balance of dioxin pollution in Lake Shinji Basin, Japan.
548 *Environ. Sci. Technol.* 35, 1967-1973.

549 McKay, G., 2002. Dioxin characterisation, formation and minimisation during municipal solid
550 waste (MSW) incineration: review. *Chem. Eng. J.* 86, 343-368.

551 Mohan, D., Sarswat, A., Ok, Y.S., Pittman, C.U., 2014. Organic and inorganic contaminants
552 removal from water with biochar, a renewable, low cost and sustainable adsorbent - A
553 critical review. *Bioresource Technol.* 160, 191-202.

554 Moon, H.B., Yoon, S.P., Jung, R.H., Choi, M., 2008. Wastewater treatment plants (WWTPs)
555 as a source of sediment contamination by toxic organic pollutants and fecal sterols in a
556 semienclosed bay in Korea. *Chemosphere* 73, 880-889.

557 Oen, A.M.P., Janssen, E.M.L., Cornelissen, G., Breedveld, G.D., Eek, E., Luthy, R.G., 2011.
558 In situ measurement of PCB pore water concentration profiles in activated carbon-
559 amended sediment using passive samplers. *Environ. Sci. Technol.* 45, 4053-4059.

560 Payne, R.B., Ghosh, U., May, H.D., Marshall, C.W., Sowers, K.R., 2019. A Pilot-Scale Field
561 Study: In Situ Treatment of PCB-Impacted Sediments with Bioamended Activated
562 Carbon. *Environmental Science & Technology* 53, 2626-2634.

563 Prisciandaroa, M., Piemonteb, V., di Celsoc, G.M., Ronconid, S., Capocelli, M., 2017.
564 Thermodynamic features of dioxins' adsorption. *J. Hazard. Mater.* 324, 645-652.

565 Sallach, J.B., Crawford, R., Li, H., Johnston, C.T., Teppen, B.J., Kaminski, N.E., Boyd, S.A.,
566 2019. Activated carbons of varying pore structure eliminate the bioavailability of 2,3,7,8-
567 tetrachlorodibenzo-p-dioxin to a mammalian (mouse) model. *Sci. Total Environ.* 650,
568 2231-2238.

569 Samuelsson, G.S., Raymond, C., Agrenius, S., Schaanning, M., Cornelissen, G., Gunnarsson,

570 J.S., 2017. Response of marine benthic fauna to thin-layer capping with activated carbon
571 in a large-scale field experiment in the Grenland fjords, Norway. *Environmental Science*
572 *and Pollution Research* 24, 14218-14233.

573 Shiu, W.Y., Doucette, W., Gobas, F.A.P.C., Andren, A., Mackay, D., 1988. Physical-chemical
574 properties of chlorinated dibenzo-p-dioxins. *Environ. Sci. Technol.* 22, 651-658.

575 Stedtfeld, R.D., Sallach, J.B., Crawford, R.B., Stedtfeld, T.M., Williams, M.R., Waseem, H.,
576 Johnston, C.T., Li, H., Teppen, B.J., Kaminski, N.E., Boyd, S.A., Tiedje, J.M., Hashsham,
577 S.A., 2017. TCDD administered on activated carbon eliminates bioavailability and
578 subsequent shifts to a key murine gut commensal. *Appl. Microbiol. Biotechnol.* 101,
579 7409-7415.

580 Tu, Y.J., Chang, C.K., You, C.F., Wang, S.L., 2012. Treatment of complex heavy metal
581 wastewater using a multi-staged ferrite process. *J. Hazard. Mater.* 209-210, 379-384.

582 Tu, Y.J., Lo, S.C., You, C.F., 2015. Selective and fast recovery of neodymium from seawater
583 by magnetic iron oxide Fe₃O₄. *Chem. Eng. J.* 262, 966-972.

584 Tu, Y.J., You, C.F., Chang, C.K., Wang, S.L., 2013. XANES evidence of arsenate removal
585 from water with magnetic ferrite. *J. Environ. Manage.* 120, 114-119.

586 USEPA, 1997. Rules of thumb for Superfund remedy selection; EPA 540-R-97-013, OSWER
587 9355.0-69, PB97-963301; U.S. Environmental Protection Agency: Washington, DC.

588 Van den Berg, M., Birnbaum, L., Bosveld, A.T.C., Brunstrom, B., Cook, P., Feeley, M., Giesy,

589 J.P., Hanberg, A., Hasegawa, R., Kennedy, S.W., Kubiak, T., Larsen, J.C., van Leeuwen,
590 F.X.R., Liem, A.K.D., Nolt, C., Peterson, R.E., Poellinger, L., Safe, S., Schrenk, D., Tillitt,
591 D., Tysklind, M., Younes, M., Waern, F., Zacharewski, T., 1998. Toxic equivalency
592 factors (TEFs) for PCBs, PCDDs, PCDFs for humans and wildlife. *Environmental Health*
593 *Perspectives* 106, 775-792.

594 WHO, 2010. Exposure to dioxins and dioxin-like substances: a major public health concern.
595 <http://www.who.int/ipcs/features/dioxins.pdf>.

596 Zhang, Q.L., Lin, Y.C., Chen, X., Gao, N.Y., 2007. A method for preparing ferric activated
597 carbon composites adsorbents to remove arsenic from drinking water. *J. Hazard. Mater.*
598 148, 671-678.

599 Zhang, S.J., Li, X.Y., Chen, J.P., 2010. Preparation and evaluation of a magnetite-doped
600 activated carbon fiber for enhanced arsenic removal. *Carbon* 48, 60-67.

601 Zhao, Y.Y., Zhan, J.Y., Liu, G.R., Zheng, M.H., Jin, R., Yang, L.L., Hao, L.W., Wu, X.L.,
602 Zhang, X., Wang, P., 2017. Evaluation of dioxins and dioxin-like compounds from a
603 cement plant using carbide slag from chlor-alkali industry as the major raw material. *J.*
604 *Hazard. Mater.* 330, 135-141.

605 Zheng, G.J., Leung, A., Jiao, L.P., 2008. Polychlorinated dibenzo-p-dioxins and diben-
606 zofurans pollution in China: sources, environmental levels and potential human health
607 impacts. *Environ. Int.* 34, 1050-1061.

608 Zhou, X.J., Buekens, A., Li, X.D., Ni, M.J., Cen, K.F., 2016. Adsorption of polychlorinated
609 dibenzo-p-dioxins/dibenzofurans on activated carbon from hexane. *Chemosphere* 144,
610 1264-1269.

611

612

613

614 Table titles:

615 Table 1. Selected physical properties of GAC, GAC-Fe₃O₄ and PAC.

616 Table 2. Kinetic parameters at different concentration for adsorption of DD by using DSRA

617 and GAC-Fe₃O₄ composite.

618

619 Figure Captions

620 Fig. 1. Saturation magnetization of GACs and PAC-Fe₃O₄ composites measured by SQUID.

621 Fig. 2. X-ray powder diffraction (XRD) patterns of the GAC-Fe₃O₄(B) and PAC-Fe₃O₄(A)

622 composites along with reference reflections for magnetite Fe₃O₄.

623 Fig. 3. Scanning electron microscopy (SEM) images of (a) DSRA (120X magnitude); (b)

624 DSRA (500X magnitude); (c) DSRA (800X magnitude); (d) GAC-Fe₃O₄ composite

625 (50000X magnitude); (e) GAC-Fe₃O₄ composite (150000X magnitude); and (f) GAC-

626 Fe₃O₄ composite (350000X magnitude).

627 Fig. 4. Batch equilibrium sorption isotherms of dibenzo-p-dioxin (DD) on GAC (black
628 squares) and GAC-Fe₃O₄(B) (red circles). Conditions: T=298 K, solution volume=30
629 mL, adsorbent =2.5 mg, contact time=10-48 h.

630 Fig. 5. Sorption kinetics of dibenzo-p-dioxin (DD) uptake by GAC and GAC-Fe₃O₄(B) over
631 40 h of contact. Top figure shows results from initial concentration of 0.8 mg/L,
632 middle figure shows results from initial concentration of 0.4 mg/L, and lower figure
633 shows initial concentration of 0.18 mg/L. GAC is represented by black squares and
634 GAC-Fe₃O₄(B) is represented by red circles. Conditions: T=298 K, solution
635 volume=30 mL, adsorbent =2.5 mg.

636 Fig. 6. Sorption kinetics of dibenzo-p-dioxin (DD) uptake by GAC, GAC-Fe₃O₄(B), PAC and
637 PAC-Fe₃O₄(A) over 18 h of contact. PAC is represented by black squares, PAC-
638 Fe₃O₄(A) is represented by solid red circles, GAC is represented by open black
639 squares, and GAC-Fe₃O₄(B) is represented by open red circles. Conditions: T=298 K,
640 solution volume=30 mL, adsorbent =2.5 mg. Conditions: DD concentration=0.8
641 mg/L, T=298 K, solution volume=30 mL, adsorbent=2.5 mg, contact time=1 h.

642

1 Figure Captions

2 Fig. 1. Saturation magnetization of GACs and PAC-Fe₃O₄ composites measured by SQUID.

3 Fig. 2. X-ray powder diffraction (XRD) patterns of the GAC-Fe₃O₄(B) and PAC-Fe₃O₄(A)
4 composites along with reference reflections for magnetite Fe₃O₄.

5 Fig. 3. Scanning electron microscopy (SEM) images of (a) DSRA (120X magnitude); (b)
6 DSRA (500X magnitude); (c) DSRA (800X magnitude); (d) GAC-Fe₃O₄ composite
7 (50000X magnitude); (e) GAC-Fe₃O₄ composite (150000X magnitude); and (f) GAC-
8 Fe₃O₄ composite (350000X magnitude).

9 Fig. 4. Batch equilibrium sorption isotherms of dibenzo-p-dioxin (DD) on GAC (black
10 squares) and GAC-Fe₃O₄(B) (red circles). Conditions: T=298 K, solution volume=30
11 mL, adsorbent =2.5 mg, contact time=10-48 h.

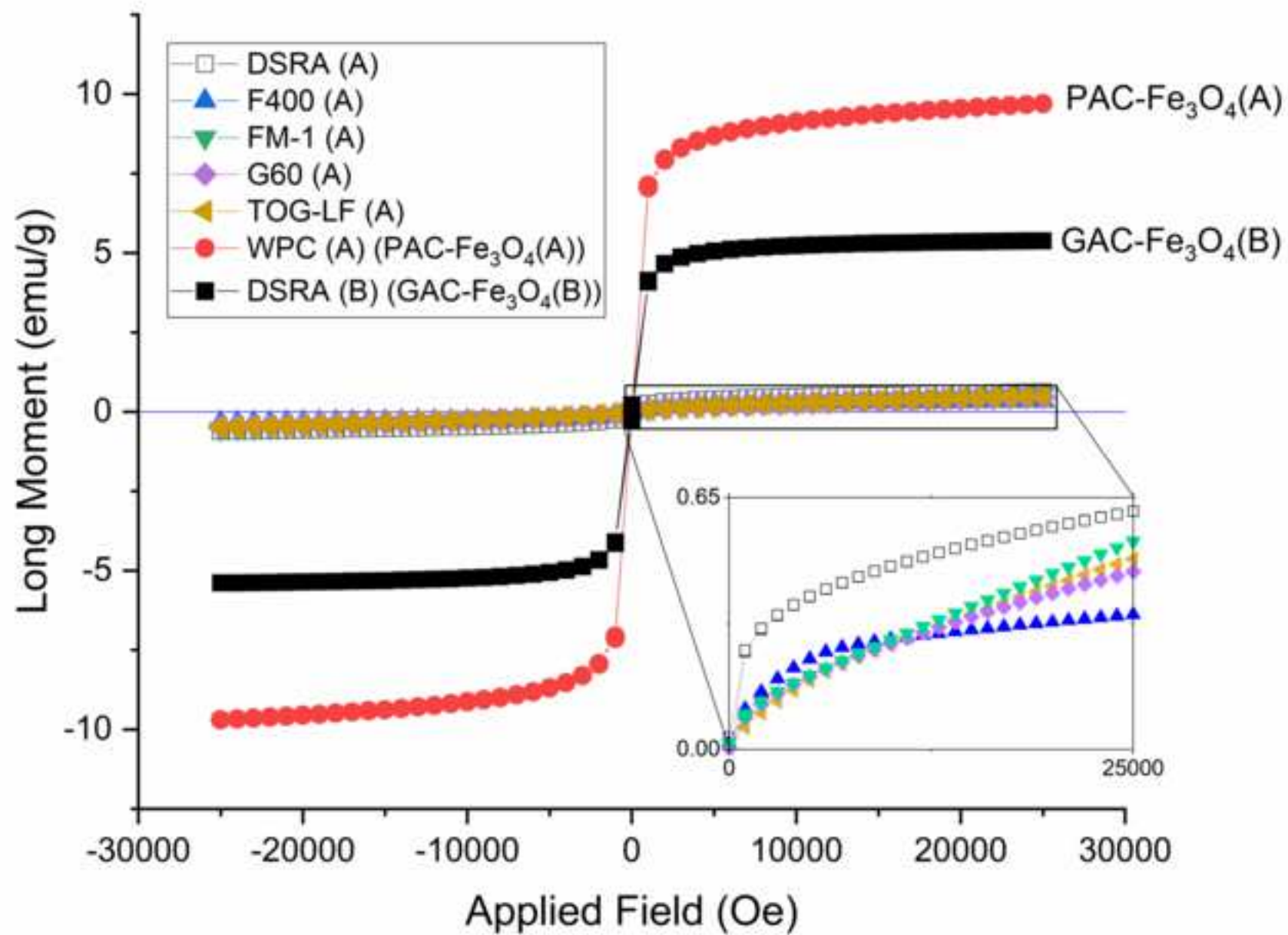
12 Fig. 5. Sorption kinetics of dibenzo-p-dioxin (DD) uptake by GAC and GAC-Fe₃O₄(B) over
13 40 h of contact. Top figure shows results from initial concentration of 0.8 mg/L,
14 middle figure shows results from initial concentration of 0.4 mg/L, and lower figure
15 shows initial concentration of 0.18 mg/L. GAC is represented by black squares and
16 GAC-Fe₃O₄(B) is represented by red circles. Conditions: T=298 K, solution
17 volume=30 mL, adsorbent =2.5 mg.

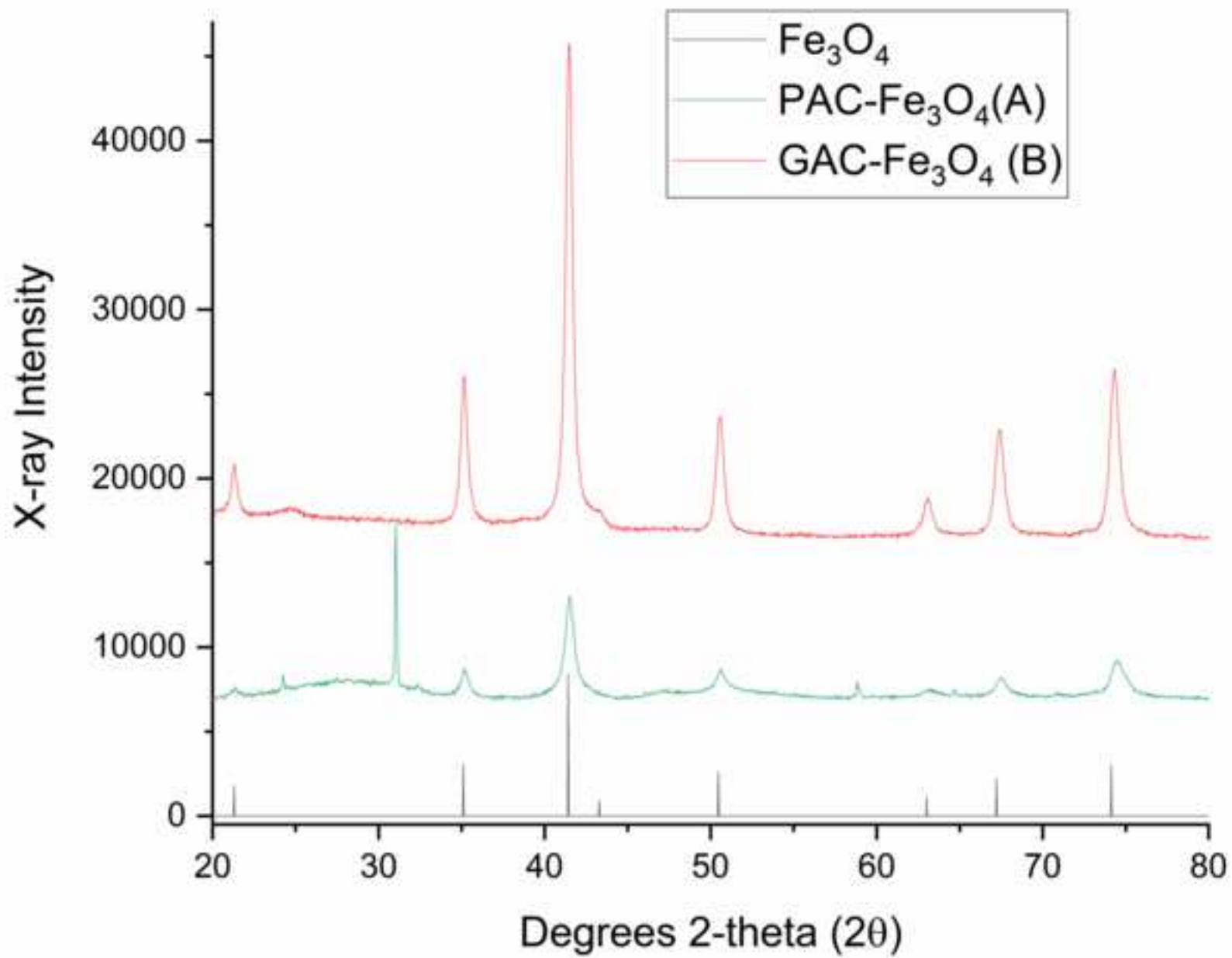
18 Fig. 6. Sorption kinetics of dibenzo-p-dioxin (DD) uptake by GAC, GAC-Fe₃O₄(B), PAC and
19 PAC-Fe₃O₄(A) over 18 h of contact. PAC is represented by black squares, PAC-

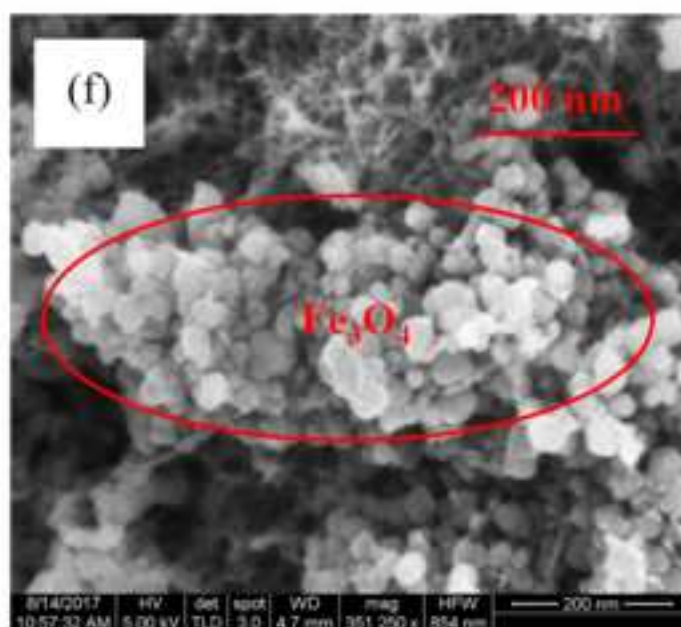
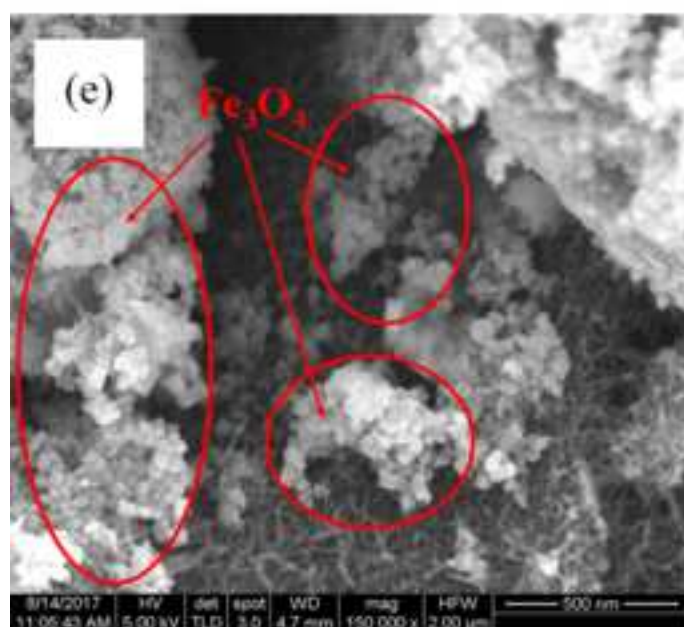
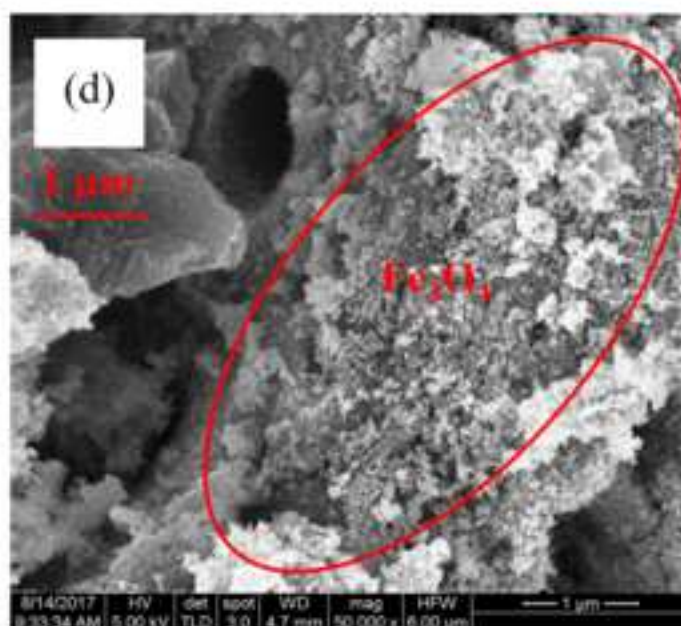
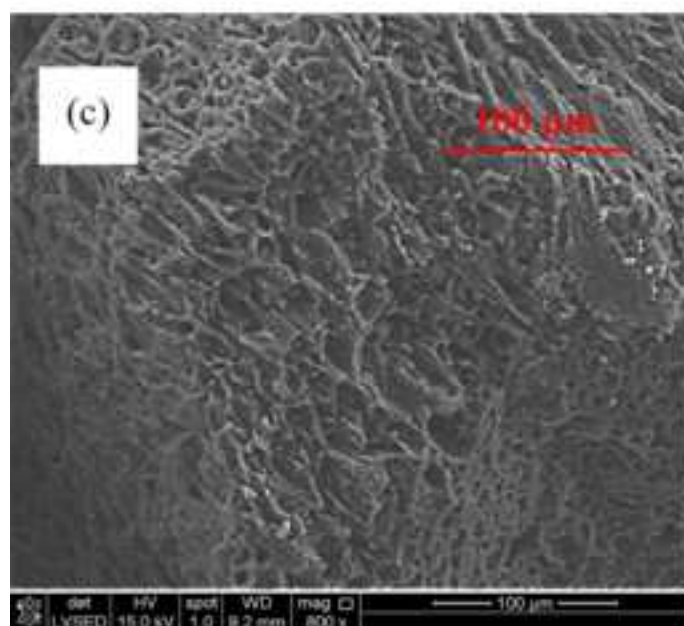
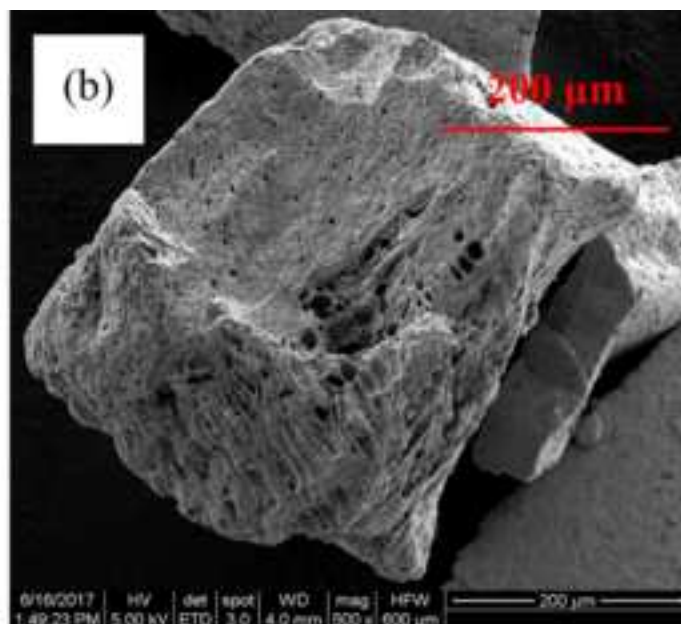
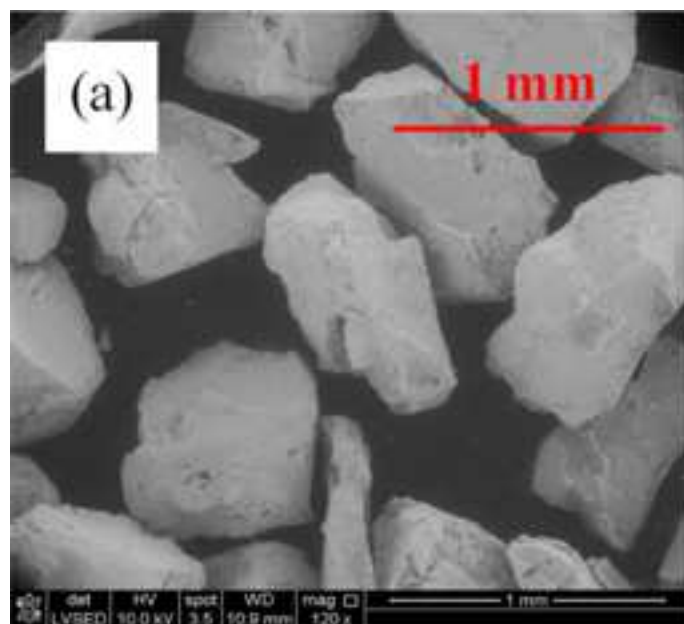
20 $\text{Fe}_3\text{O}_4(\text{A})$ is represented by solid red circles, GAC is represented by open black
21 squares, and GAC- $\text{Fe}_3\text{O}_4(\text{B})$ is represented by open red circles. Conditions: $T=298\text{ K}$,
22 solution volume=30 mL, adsorbent =2.5 mg. Conditions: DD concentration=0.8
23 mg/L, $T=298\text{ K}$, solution volume=30 mL, adsorbent=2.5 mg, contact time=1 h.

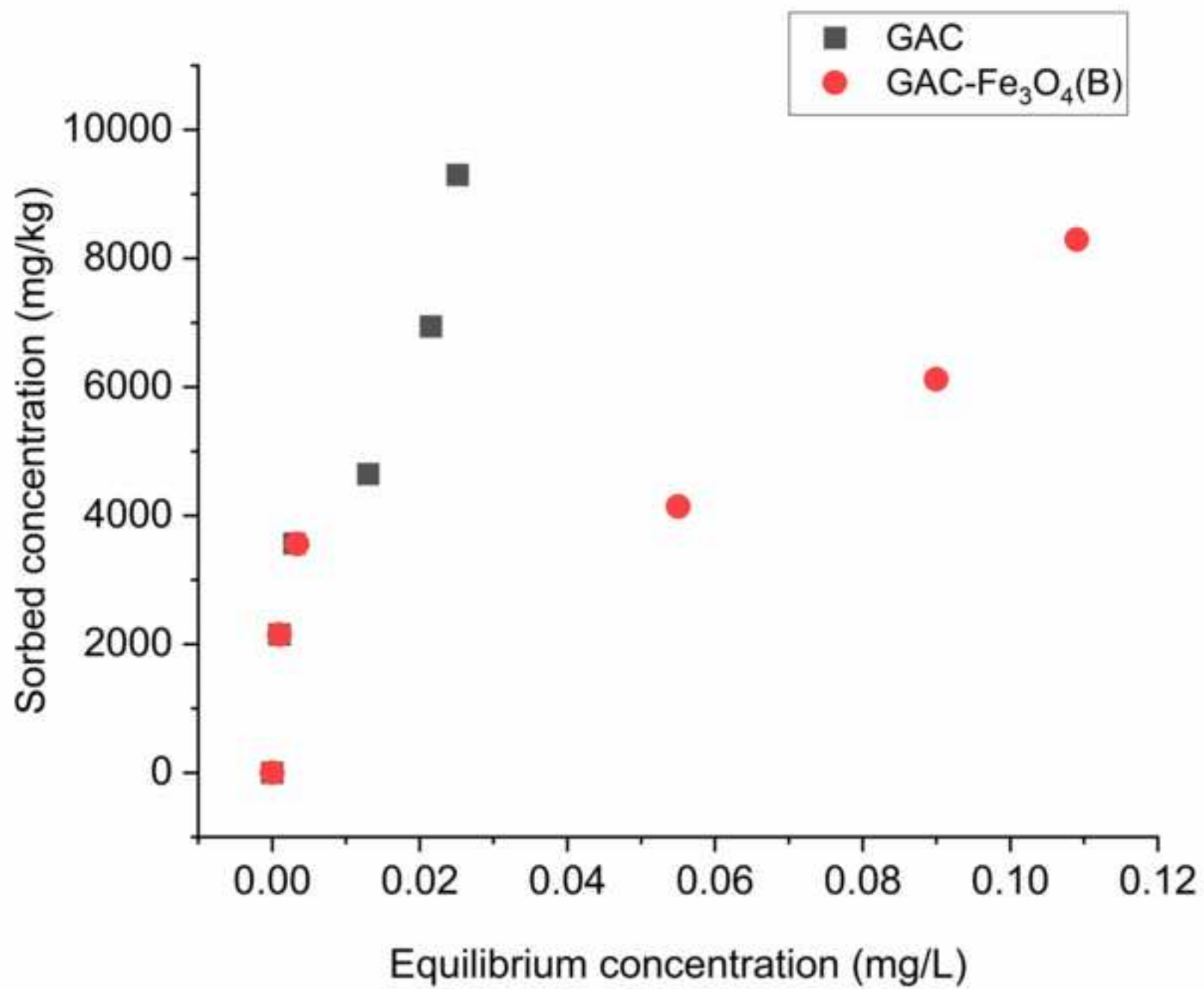
24

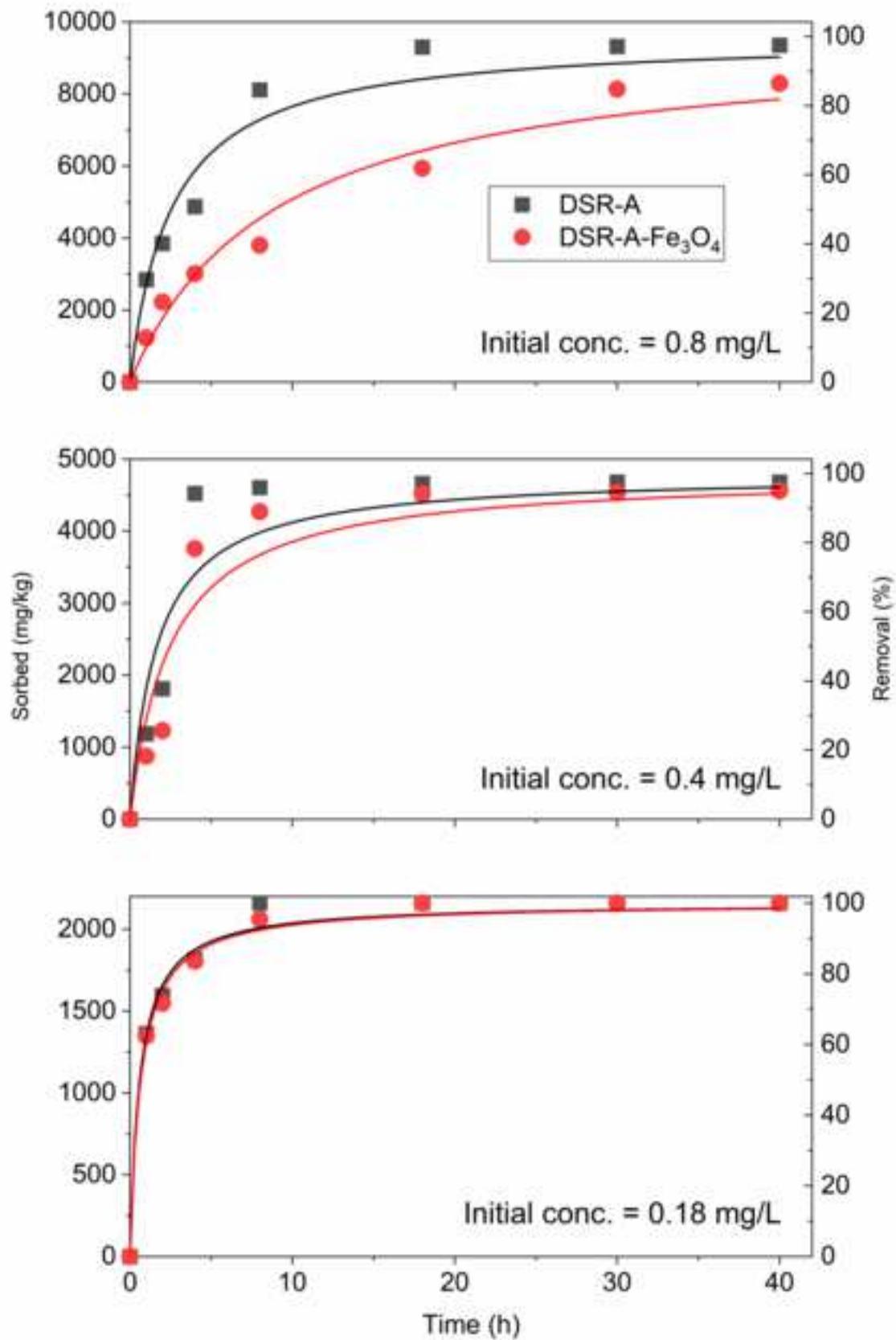
25











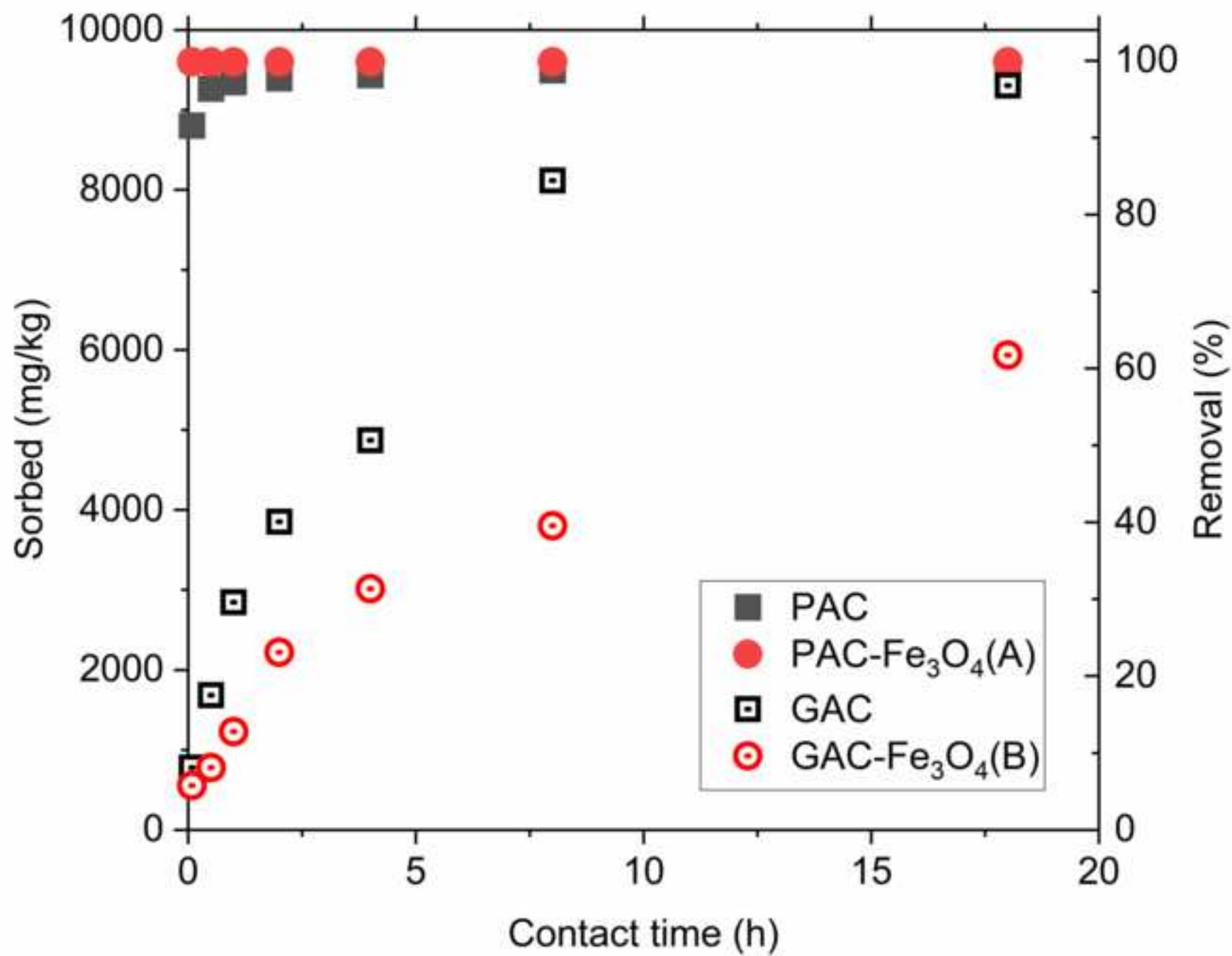


Table 1. Selected physical properties of the activated carbon materials

Material	Supplier	Source	Surface Area (m ² /g)	Mesopore vol. g/cc (% of total)	Micropore vol. g/cc (% of total)	^a Magnetization after Syn. Method A (emu/g)	^b Magnetization after Syn. Method B (emu/g)
G60	Cabot	Lignite	987	0.38 (57%)	0.29 (43%)	0.46	
FM-1	Cabot	Lignite	520	0.36 (71%)	0.15 (29%)	0.54	
TOG-LF	Calgon	Coal	916	0.15 (33%)	0.30 (67%)	0.49	
F-400	Calgon	Coal	1044	0.16 (31%)	0.36 (69%)	0.35	
WPC (AC)	Calgon	Coconut	802	0.03 (9%)	0.29 (91%)	9.7	
DSRA (GAC)	Calgon	Pool Rej.	822	0.11 (22%)	0.38 (78%)	0.61	
DSRA-Fe ₃ O ₄	Calgon	Pool Rej.	633	0.06 (18%)	0.26 (82%)		5.38

Note:

^a: Magnetization after Fe₃O₄ impregnation at conditions of 338 K and 0.01 M FeSO₄.

^b: Magnetization after Fe₃O₄ impregnation at conditions of 298 K and 0.1 M FeSO₄.

Table 2. The pseudo-second order kinetic model for GAC (DSRA) and GAC-Fe₃O₄(B)

	GAC (DSRA)			GAC-Fe ₃ O ₄ (B)		
	q _e	k ₂	Adjusted R Square	q _e	k ₂	Adjusted R Square
0.18 mg/L	2160	7.62E-04	0.990	2160	7.02E-04	0.994
0.4 mg/L	4800	1.26E-04	0.893	4800	8.47E-05	0.916
0.8 mg/L	9600	4.10E-05	0.967	9600	1.17E-05	0.973